Journal of Sustainable Development of Energy, Water and Environment Systems

http://www.sdewes.org/jsdewes

Year 2026, Volume 14, Issue 4, 1140741,

Original Research Article

From Resource Complementarity to Temporal Integration Behaviour: A Technology-Agnostic Framework for Wind–Solar Hybrid Systems

Miranda Halili*[1], Valbona Muda[2], Driada Mitrushi[2], Fjorela Verore[3]

[1]University of Vlora "Ismail Qemali", Faculty of Technical and Natural Sciences, Department of Engineering and Maritime Technology,58 Kosova Street, Vlora 9400, Albania,

[2]Polytechnic University of Tirana, Faculty of Mathematical and Physical Engineering, Department of Physical Engineering, Mother Teresa Square, Tirana 1001, Albania,

[3]University of Vlora "Ismail Qemali", Faculty of Technical and Natural Sciences, Department of Mathematics and Physics, 58 Kosova Street, Vlora 9400, Albania,

e-mail: miranda.halili@univlora.edu.al, v.muda@fimif.edu.al, d.mitrushi@fimif.edu.al, fjorela.verore@univlora.edu.al

Cite as: Halili, M., Muda, V., Mitrushi, D., Verore, F., From Resource Complementarity to Temporal Integration Behaviour: A Technology-Agnostic Framework for Wind–Solar Hybrid Systems, J.sustain. dev. energy water environ. syst., 14(4), 1140741, 2026, DOI: https://doi.org/10.13044/j.sdewes.d14.0741

ABSTRACT

This study presents a technology-agnostic framework for analysing wind–solar hybridisation from a resource-based perspective, focusing on integration-relevant temporal behaviour. Renewable availability is represented using normalised signals, enabling the evaluation of variability and inter-period transition intensity as key indicators of temporal dynamics. The results reveal a non-linear response to the mixing parameter, with variability minimised at balanced wind–solar contributions, while transition intensity reaches its minimum at higher solar shares. This non-coincidence highlights an inherent trade-off between different integration objectives. A demand-aware residual proxy is introduced to assess temporal alignment between renewable availability and electricity demand, indicating improved alignment under hybrid configurations at monthly resolution. The framework operates independently of technology-specific assumptions and dispatch modelling, providing a transparent basis for early-stage planning and hybrid configuration screening. The findings demonstrate how resource complementarity can be systematically linked to integration-relevant behaviour across temporal scales.

KEYWORDS

Wind–solar hybrid systems; Resource complementarity; Temporal variability; Inter-period transition; Demand–availability alignment; Technology-agnostic framework; Renewable energy integration.

INTRODUCTION

The large-scale integration of variable renewable energy sources has fundamentally altered the operational paradigm of modern power systems, shifting the primary challenge from long-term energy adequacy to short-term flexibility and integration-related stability requirements. In contrast to conventional dispatchable generation, wind and solar resources are characterised by pronounced temporal variability and limited controllability, resulting in recurrent periods of low availability and temporal fluctuations [1]. As renewable penetration increases, these dynamics evolve from secondary considerations into dominant operational constraints. Power

* Corresponding author

systems are therefore required to manage higher levels of short-term variability while maintaining reliability, often leading to an increased dependence on reserve capacity, flexibility options, and energy storage solutions [2]. Long-term storage requirements in systems with high shares of variable renewable energy have been shown to depend strongly on the temporal variability of renewable supply [3], while recent planning studies further emphasise the role of variability in shaping storage needs and overall system design [4]. In this context, the ability to stabilise aggregate renewable supply across multiple temporal scales constitutes a critical determinant of successful renewable energy integration. In this study, stability is considered in a proxy-based and planning-oriented sense, focusing on integration-relevant characteristics of renewable availability rather than classical power system stability phenomena, such as frequency or voltage stability. Specifically, it refers to statistical properties of renewable availability that are relevant for system integration, including variability, inter-period transitions, and demand–availability alignment. These indicators should be interpreted as proxies of integration-relevant behaviour rather than direct measures of power system stability.

Accordingly, the proposed framework captures stability-related behaviour at the resource level, rather than operational system dynamics governed by grid physics and control mechanisms. It is therefore important to distinguish between grid-level stability, which involves frequency and voltage regulation, and the resource-level indicators adopted in this study. These indicators describe the ability of combined renewable resources to produce a more temporally consistent and predictable availability profile prior to any active grid intervention or compensation.

Building on this conceptual distinction, flexibility requirements associated with high shares of variable renewable energy have been extensively investigated through both planning and operational modelling frameworks, which capture system behaviour across multiple temporal scales [5]. A persistent challenge in this literature is the mismatch between the temporal resolution of power system operations and that of long-term energy planning. While operational studies typically rely on high-resolution (hourly or sub-hourly) time series to capture short-term dynamics, long-term assessment models often employ aggregated temporal representations that smooth out variability [6], a limitation that has been explicitly highlighted in integrated assessment modelling studies [7]

To address this limitation, several modelling approaches have sought to explicitly incorporate high-resolution renewable variability into long-term assessment frameworks, thereby improving the representation of temporal dynamics and system constraints [8].

More recently, high-resolution climate reanalysis has been shown to be essential for capturing the nuanced global patterns of wind–solar complementarity, providing a robust basis for hybrid renewable energy system design [9]. Within this broader integration context, wind–solar hybridisation has attracted increasing attention as a strategy for mitigating the variability inherent in individual renewable resources. Owing to their asynchronous temporal behaviour, wind and solar resources can partially compensate for each other, leading to smoother aggregate availability profiles. Recent studies have adopted portfolio-based perspectives to address variability and supply risk, highlighting the importance of technological, spatial, and temporal complementarities in reducing variability at the system level [10]. In addition, the role of complementarity and resource variability characteristics in shaping hybrid system performance under varying climatic conditions has been increasingly emphasised [11].

In the Mediterranean context, the co-location of wind and solar resources has been shown to improve energy yield and reduce variability through complementary temporal behaviour, thereby enhancing the integration potential of hybrid renewable systems [12].

Despite these advances, most existing studies remain primarily descriptive, focusing on correlation structures, complementarity indices, or resource co-variability without explicitly linking these properties to system-relevant outcomes [13], [14], [15]. In particular, recent reviews have highlighted that existing complementarity metrics are unable to capture all relevant dimensions of resource interaction and often provide only partial representations of

system behaviour [16]. More broadly, the integration of variable renewable energy sources into power systems continues to present key challenges related to variability, uncertainty, and system flexibility requirements [17], [18]. Within the planning-oriented context adopted in this study, inter-period transition intensity is defined as the mean absolute first-order difference of the availability signal. In parallel, hybrid renewable energy system studies frequently incorporate storage or auxiliary technologies [19], [20], [21]. While these approaches demonstrate practical feasibility, they typically rely on technology-specific assumptions, such as installed capacities, dispatch strategies, or system configurations, which limits their transferability to early-stage planning contexts.

More recent contributions have introduced demand-aware perspectives, for example through residual load analysis, to better capture system-relevant dynamics [22]. However, these approaches remain dependent on detailed system representations and do not provide a generalised framework that is not tied to specific technological configurations.

Consequently, a clear methodological gap persists between descriptive resource complementarity analysis and integration-oriented system-level assessment, as existing studies remain fragmented and lack a unified, technology-agnostic framework linking resource-level interactions to system-level behaviour. This highlights the need for analytical approaches that can establish such a linkage in a transparent and transferable manner.

Building on this gap, the present study develops a technology-agnostic analytical framework for wind–solar hybridisation, based on normalised resource availability signals that preserve temporal structure while enabling consistent cross-resource evaluation.

These signals are combined through a continuous mixing parameter (α), enabling systematic exploration of hybrid configurations without reliance on technology-specific assumptions. The parameter α is interpreted as a dimensionless resource-level mixing factor rather than a direct representation of installed capacity or generation shares. Accordingly, the framework is intended for exploratory and screening purposes rather than direct system design. Integration-relevant system-level behaviour is evaluated using multiple metrics, including variability, inter-period transition intensity, and low-availability events, complemented by a demand-aware residual-based proxy [23].

The key contribution of this study is the explicit identification of distinct and non-coincident integration mechanisms governing wind–solar hybrid systems, demonstrating that optimal configurations differ across variability, transition behaviour, and low-availability conditions.

The novelty of the proposed approach lies in the explicit integration and analytical interpretation of multiple stability-relevant dimensions within a unified, generalised analytical framework, rather than treating them as independent or implicitly aligned indicators. By linking resource-level complementarity to system-level behaviour across temporal scales, the study moves beyond purely descriptive analyses and establishes a coherent basis for stability-oriented screening in early-stage renewable energy planning.

To enhance the robustness and generalisability of the proposed framework, the analysis is conducted across three distinct climatic zones in Albania: the Coastal Belt, the Western Lowlands (represented by the Vlorë case study), and the Mountainous Area. The analysis is performed at a monthly temporal resolution, consistent with its planning-oriented objective. For the multi-zonal assessment, high-resolution hourly time-series data are initially processed and subsequently aggregated, ensuring that the underlying temporal structure of resource variability is preserved prior to evaluation**.** This multi-scale temporal approach, combined with geospatial validation, enables the framework to capture diverse resource dynamics and provides transferable insights for hybrid renewable system design in regions characterised by strong seasonal variability.

Overall, the study establishes a direct analytical linkage between resource-level complementarity and multiple integration-relevant stability dimensions, offering a generalisable and transferable framework for hybrid renewable system assessment.

METHODS

This section presents the proposed analytical framework for evaluating wind–solar hybridisation from a system-integration perspective. The approach is designed to quantify integration-relevant, planning-oriented stability characteristics using transparent, technology-neutral metrics derived from normalised resource availability signals. These metrics should be interpreted as proxy indicators of temporal behaviour relevant for renewable energy integration, rather than as direct measures of operational power system stability.

By abstracting from technology-specific parameters, such as installed capacity, conversion efficiency, and dispatch strategies, the framework isolates the underlying climatic potential for temporal balancing, thereby ensuring robustness across different technological configurations and geographic contexts. The overall structure of the analytical framework is illustrated in Figure 1. The approach proceeds sequentially from data acquisition and normalisation to hybrid signal construction and multi-dimensional assessment of integration-relevant temporal behaviour. Central to the framework is a continuous mixing parameter (α), which is used to combine normalised wind and solar availability indices into a composite hybrid signal $H(t)$. The parameter α is defined as a dimensionless analytical weighting factor and does not represent installed capacity, generation share, or any physical system configuration. Instead, it enables a systematic exploration of the relative contribution of wind and solar availability within a generalised analytical framework.

To enhance the generalisability of the analysis and address the limitations of single-site studies, the framework is applied across three distinct topographic archetypes in Albania: the Coastal Belt, the Western Lowlands (represented by the Vlora reference site), and the Mountainous Area. This multi-zonal implementation allows the identification of stability-relevant mixing regimes under heterogeneous climatic conditions and supports the evaluation of the robustness of the framework across different resource contexts.

The core analysis is conducted on monthly aggregated time series for the Vlora case study. In the multi-zonal analysis, high-resolution hourly ERA5 data are initially used to capture underlying temporal variability and ensure statistical robustness. These time series are subsequently aggregated to monthly values prior to the evaluation of the stability metrics.

This temporal aggregation is intentionally adopted and aligned with the strategic objective of the framework, which focuses on medium- to long-term variability patterns rather than short-term operational dynamics. All metrics are therefore evaluated at a monthly temporal resolution, and the results should be interpreted within this aggregation level. The framework is designed as a resource-level screening tool and does not aim to represent high-frequency system dynamics or operational balancing processes.

The framework follows a structured five-stage procedure:

1. Input data acquisition. High-resolution ERA5 atmospheric reanalysis data (approximately 10 × 10 km spatial resolution) are utilised to characterise wind speed (at 100 m hub height) and solar (surface solar radiation downwards, SSRD) resource availability. The data are used to construct consistent time series aligned with the temporal scope of the analysis.

2. Normalisation. Raw meteorological time series are transformed into standardised availability indices using Z-score normalisation. This transformation removes differences in physical units and magnitude, enabling consistent comparison between wind and solar resources. The resulting indices represent relative temporal deviations from their long-term mean and do not correspond to energy production or resource magnitude. The purpose of this step is to isolate temporal variability and co-variability patterns within a technology-agnostic framework.

3. Hybrid signal construction. A composite availability signal is constructed by combining the normalised solar and wind indices through the continuous mixing parameter α. This formulation allows hybridisation to be analysed as an emergent property of resource

availability, without imposing assumptions on system configuration or technology performance.

4. Stability metric evaluation. Integration-relevant temporal behaviour is evaluated using statistical indicators derived from the availability signals. These include variability (standard deviation), inter-period transition intensity (defined as the mean absolute first-order difference between consecutive time steps), and low-availability event frequency. These indicators are interpreted as proxy measures of temporal consistency and variability at the planning scale, and do not represent operational metrics such as ramp rates, reserve requirements, or system reliability indices.

5. Optimisation and trade-off analysis: Stability-optimal configurations are identified by analysing the dependence of the metrics on the mixing parameter α. This parametric evaluation enables the exploration of trade-offs between variability reduction, inter-period transitions, and demand-alignment potential, highlighting the multi-dimensional nature of hybrid system behaviour.

Figure 1 provides an overview of the workflow of the proposed framework, illustrating the progression from input data and normalisation to hybrid signal construction, stability metric assessment, and optimal mix determination.

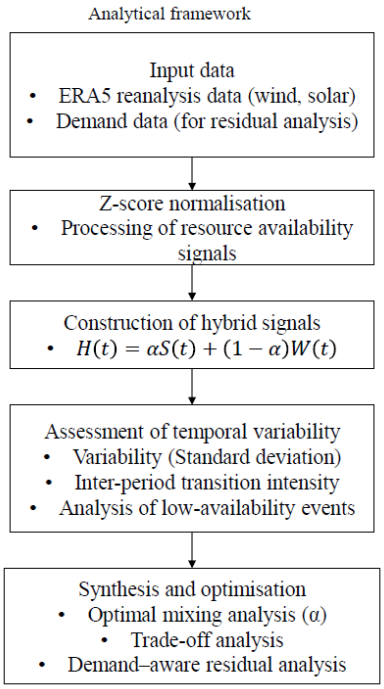

Figure 1. Workflow of the proposed technology-agnostic framework for evaluating variability- and transition-based characteristics of wind–solar hybrid availability using the mixing parameter (α), where $S(t)$, $W(t)$, and $H(t)$ denote the normalised solar, wind, and hybrid availability signals, respectively.

In the multi-zonal implementation, all stability metrics are computed independently for each topographic archetype and subsequently compared to assess the consistency of stability-optimal mixing regimes across different climatic conditions.

Data acquisition and spatiotemporal resolution

The data sources and spatiotemporal resolution adopted for the analysis are outlined below.

The primary climatic inputs for this study were obtained from the ERA5 atmospheric reanalysis dataset [24], developed by the European Centre for Medium-Range Weather Forecasts (ECMWF) and accessed via the Copernicus Climate Data Store [25]. ERA5 provides long-term, spatially and temporally consistent meteorological data and is widely used in renewable energy resource assessment and system integration studies.

To ensure adequate spatial representation and enhance the generalisability of the analysis, a high-resolution grid of approximately 10 × 10 km (≈0.1° × 0.1°) was employed. This spatial resolution enables the representation of regional climatic variability and topographic influences across Albania's heterogeneous terrain.

Hourly time series for wind speed (at a hub height of 100 m) and surface solar radiation downwards (SSRD), covering the period 2014–2024, were extracted and processed using QGIS 3.40 Bratislava [26]. The spatial delineation of the three topographic archetypes was based on high-resolution vector datasets (1:10m scale) obtained from Natural Earth [27].

To capture the influence of topography and meteorological variability, the study area was stratified into three distinct physiographic archetypes. This spatial classification, illustrated in Figure 2, was derived from a high-resolution Digital Elevation Model (DEM) and processed within a GIS environment to ensure altimetry accuracy. The territory was delineated into the Coastal Belt (0–20 m), Western Lowlands (20–200 m), and Mountainous Area (>200 m), accounting for differences in surface roughness and orographic effects that influence wind and solar resource patterns. This approach enables a transition from a localised analysis to a multi-zonal assessment, reducing site-specific bias and improving the transferability of the results.

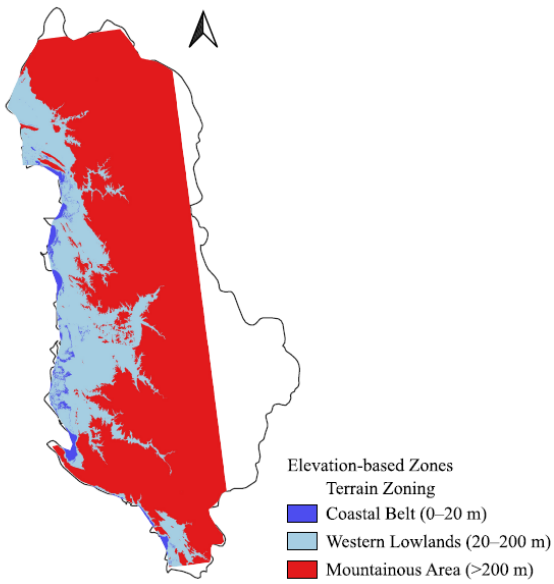

Figure 2. Elevation-based classification of the study area (Albania), defining three topographic archetypes: Coastal Belt (0–20 m), Western Lowlands (20–200 m), and Mountainous Area (>200 m).

The methodological framework operates across two complementary temporal perspectives in order to balance statistical robustness with planning-oriented interpretability.

(i) Strategic case study analysis: For the Vlora reference site, representing the Western Lowlands, hourly data were aggregated to a monthly temporal resolution. This aggregation is intentionally adopted to emphasise long-term seasonal variability patterns and inter-period transitions, which are relevant for planning-stage assessments and high-level system integration analysis.

(ii) Multi-zonal validation: To extend the analysis beyond a single-site application and evaluate the spatial robustness of the framework, the full hourly ERA5 dataset was analysed across three topographic archetypes: the Coastal Belt (low-elevation maritime grid cells), the

Western Lowlands (transitional plains), and the Mountainous Area (high-elevation inland regions).

To maintain methodological consistency between the case study and the spatial validation, all results are evaluated at a common monthly temporal resolution. While the Vlora case study uses directly aggregated monthly data, the multi-zonal analysis is initially performed at hourly resolution and subsequently aggregated to monthly values prior to the construction of the normalised availability indices. This approach preserves the underlying temporal variability while ensuring consistency in comparative assessment. This temporal resolution is intentionally selected to support planning-stage analysis, focusing on medium- to long-term variability patterns and inter-period transitions, and should not be interpreted as representing short-term operational system behaviour.

Resource normalization and standardization.

This section describes the normalisation approach adopted to ensure comparability between wind and solar resource signals. To enable a consistent comparison between wind speed (m/s) and solar irradiance (W/m²), which differ in both physical units and statistical distributions, a normalisation step is required prior to any joint analysis. In this study, a z-score normalisation procedure is applied to transform the original meteorological time series into dimensionless availability indices. The standardised availability index is defined as:

$$z_x\ (t) = \frac{X(t) - \mu_X}{\sigma_X} \qquad (1)$$

Where $X(t)$ represents the original variable (solar irradiance or wind speed), μ_x and σ_x denote its long-term mean and standard deviation over the analysis period. The resulting indices $S(t)$ and $W(t)$ are dimensionless and centred around zero. Positive values indicate above-average resource availability and negative values indicate below-average conditions.

This transformation serves a purely statistical purpose: it removes differences in units and magnitude while preserving the temporal structure and variability patterns of each resource, thereby enabling a consistent comparison and combination within a common analytical framework.

The use of standardised anomalies is well established in climate statistics and time-series analysis [28], and has been increasingly applied in renewable energy studies to analyse variability, co-variability, and complementarity between resources [29], [30]. In particular, normalisation-based approaches are commonly used to enable cross-resource comparability and to isolate temporal variability patterns independently of magnitude effects [31], [32].

At the same time, it should be acknowledged that z-score normalisation removes information about absolute resource magnitude and potential energy yield. Consequently, reductions in variability observed in the standardised indices do not necessarily imply proportional reductions in variability of actual electricity generation. This limitation has also been highlighted in recent renewable energy studies addressing normalisation and forecasting across heterogeneous datasets [33].

Alternative normalisation approaches, such as min–max scaling or capacity-factor-based transformations, may retain partial information on magnitude or energy yield. However, these approaches introduce implicit assumptions related to resource bounds or technology performance, which would reduce the generality of the analysis. The z-score formulation is therefore adopted as a neutral statistical transformation that preserves temporal structure while avoiding technology-specific parameterisation.

Accordingly, the derived indices do not represent electricity generation or physical system performance. Rather, they should be interpreted as abstract resource availability proxies

suitable for analysing relative temporal behaviour at the planning stage, and not as direct representations of power system operation or stability in the engineering sense. By explicitly excluding technology-specific characteristics—such as turbine power curves, photovoltaic performance models, and system constraints—the framework remains intentionally independent of technology-specific modelling assumptions. Within this context, $S(t)$ and $W(t)$are used to evaluate integration-relevant statistical indicators, including variability, inter-period transition intensity, and the occurrence of low-availability conditions, rather than operational system metrics.

Hybrid signal synthesis and the mixing parameter (α)

Wind–solar complementarity is represented through a hybrid availability signal defined as a linear combination of the normalised solar and wind indices, governed by a continuous mixing parameter, α.

$$H(t) = \alpha S(t) + (1-\alpha)W(t), \qquad \alpha \in [0,1] \tag{2}$$

where α is a dimensionless continuous mixing parameter controlling the relative contribution of each resource, consistent with index-based representations of renewable resource complementarity adopted in the literature [34].

Importantly, α does not correspond to installed capacity, generation share, or a physical system configuration. Instead, it represents an abstract balancing weight that governs the relative influence of wind and solar availability within the aggregated signal.

Treating α as a continuous variable allows variability- and transition-based metrics to be evaluated as smooth functions of the mixing ratio, enabling a systematic exploration of trade-offs across the full spectrum from wind-dominated to solar-dominated regimes. In this context, α represents relative resource dominance under idealised conditions rather than a direct prescription for capacity allocation.

This formulation enables hybridisation to be analysed as an emergent property of resource availability, independent of technology-specific assumptions. Consequently, the framework provides transferable insights for early-stage planning, while recognising that translating optimal α values into real-world system configurations would require additional modelling of technological and operational constraints.

Integration-relevant variability and transition metrics

The statistical metrics used to characterise integration-relevant temporal behaviour from a resource-based perspective are defined below. The proposed framework evaluates multiple complementary indicators, including variability, inter-period transition intensity, demand-aware residual analysis, and low-availability conditions.

Variability metric. Variability is assessed using statistical metrics computed from the normalised availability signals. It is evaluated for each signal $X(t) \in \{S(t), W(t), H(t)\}$, where $S(t)$ denotes the solar availability index, $W(t)$ the wind availability index, and $H(t)$ the hybrid availability signal.

For each signal, variability is quantified using the standard deviation:

$$\sigma_X = \sqrt{\frac{1}{T-1}\sum_{t=1}^{T}[X(t)-\bar{X}]^2} \tag{3}$$

where T denotes the length of the time series and $\bar{X}$ its long-term mean. This metric captures the dispersion of availability around its mean state, with lower values indicating

reduced temporal variability and a more stable availability profile. When applied to normalised availability signals, σ_X represents a second-order statistical descriptor of temporal variability.

From a stochastic-process perspective, variance and standard deviation constitute canonical measures of dispersion and are widely used to characterise the spread of time series around their mean state [35]. Within renewable energy studies, reduced variability in aggregated availability signals is commonly interpreted as indicative of smoother temporal resource behaviour, which may influence balancing requirements and flexibility needs at a planning level [36]. However, this relationship remains indirect and should not be interpreted as a direct measure of operational system stability. Accordingly, the dependence of the hybrid variability σ_H on the mixing parameter α is analysed to identify wind–solar combinations that minimise variability relative to single-resource configurations.

Inter-period transition intensity. It is introduced as a measure of temporal changes in renewable availability. In addition to overall variability, system integration is influenced by the magnitude of fluctuations between consecutive time steps. Given the monthly temporal resolution adopted in this study, this metric captures medium-term transitions in availability rather than short-term operational inter-period transition intensity. For each availability signal $X(t) \in \{S(t), W(t), H(t)\}$, the transition intensity is defined as the absolute difference between consecutive time steps:

$$R_x(t) = |X(t) - X(t-1)| \quad (4)$$

The corresponding transition intensity is summarised by the mean absolute difference:

$$R_X = \frac{1}{T-1}\sum_{t=2}^{T} R_X(t) \quad (5)$$

where T denotes the number of time steps in the series (months).

From a time-series perspective, this metric corresponds to the absolute first-difference process of the availability signal. First differences are widely used to characterise temporal dynamics, persistence, and transition intensity in stochastic processes , [37], [38]. Metrics based on successive differences have been widely used to characterise temporal fluctuation behaviour, particularly in wind-dominated systems [39]. Given the monthly temporal resolution adopted here, the metric captures inter-period changes in availability and does not resolve short-term system dynamics. It is therefore interpreted as a measure of medium-term transition behaviour.

When applied to normalised availability indices, this metric complements the standard deviation–based variability metric by explicitly capturing the magnitude of successive temporal transitions.

In this study, the dependence of the hybrid transition intensity metric R_H on the mixing parameter α is analysed to identify wind–solar combinations that minimise inter-period variability relative to single-resource configurations

Demand-aware residual analysis. To evaluate the alignment between hybrid availability and actual consumption, a residual proxy is introduced. The residual signal $R\_X(t)$ represents the mismatch between normalised demand $D(t)$ and availability $X(t)$:

$$R\_X(t) = D(t) - X(t) \quad (6)$$

The magnitude of this mismatch is quantified through the variability of the residual signal:

$$\sigma_R = std[R_X(t)] \quad (7)$$

Lower values of σ_R indicate improved temporal alignment between renewable availability and demand.

Residual-based formulations are used to analyse demand–supply interactions in renewable-dominated systems, particularly in studies employing residual load metrics to assess complementarity and system-level effects [40]. In the present framework, the residual is interpreted as a planning-level proxy that captures temporal mismatch patterns without representing physical system balancing, dispatch processes, or operational constraints.

Low-availability events**.** Beyond overall variability and inter-period transition intensity, system integration is also affected by the occurrence of periods with persistently low renewable availability. Such conditions have been identified as critical stress periods in systems with high shares of variable renewable energy, often referred to as wind and solar energy droughts [41]. Low-availability events are identified directly from the normalised availability signals $X(t) \in \{S(t), W(t), H(t)\}$ using a percentile-based threshold. An event is defined whenever:

$$X(t) < X_p \quad (8)$$

where X_p denotes the p-th percentile of the empirical distribution of the corresponding availability signal.

From a statistical perspective, this approach characterises the lower-tail behaviour of the availability distribution. Percentile-based thresholds are commonly employed to identify rare or extreme conditions in stochastic processes, particularly when absolute magnitudes are not directly comparable across variables [42]. The relative definition ensures a consistent, dimensionless representation of scarcity across wind, solar, and hybrid configurations. Low-availability conditions are summarised using two complementary indicators:

(i) the frequency of low-availability events, expressed as the fraction of time steps below the threshold, and

(ii) the duration of consecutive low-availability periods, which captures the persistence of scarcity conditions.

Together, these indicators provide insight into the likelihood and temporal structure of prolonged low-availability episodes, which are relevant for planning-oriented assessments of supply risk, without representing operational adequacy metrics.

Further methodological details, including the scope, assumptions, and limitations of the proposed metrics, are provided in Supplementary Material S4.

Optimal mixing analysis.

Optimal hybrid configurations are identified by analysing how integration-relevant stability metrics vary as a function of the mixing parameter α. The hybrid availability signal is constructed using the normalised indices $S(t)$ and $W(t)$, and the corresponding metrics are evaluated across the full admissible range $\alpha \in [0, 1]$. To enable a continuous assessment of hybrid configurations, the mixing parameter is sampled over a dense, and uniformly spaced grid. For each value of α, the hybrid availability signal $H(t;\alpha)$ is computed and the corresponding stability metrics are evaluated, including variability (standard deviation) and inter-period transition intensity (mean absolute first-order difference). This procedure yields continuous response functions describing the dependence of each metric on the mixing parameter.

Optimal configurations are identified by locating the minima of these metric curves, formally defined as:

$$\alpha_v = arg\ min\ \sigma\big(H(t;\alpha)\big) \qquad \alpha \in [0,1] \qquad (9)$$

$$\alpha_r = arg\ min\ mean(|\Delta H(t;\alpha)|) \qquad \alpha \in [0,1] \qquad (10)$$

where α_v corresponds to the variability-optimal configuration and α_r to the transition-intensity-optimal configuration.

Importantly, the mixing parameter α is not interpreted as a physical quantity such as installed capacity or generation share. Instead, it represents a dimensionless weighting factor that enables a continuous exploration of hybrid availability behaviour within a normalised, technology-agnostic framework. Accordingly, the identified optimal values should be interpreted as indicative of relative resource dominance (e.g., wind- or solar-leaning configurations), rather than as prescriptive system design parameters.

This parametric evaluation constitutes a sensitivity analysis of integration-relevant behaviour with respect to the mixing parameter, enabling the identification of stability-optimal regimes and the explicit characterisation of trade-offs between different metrics.

Analytical interpretation of stability trade-offs.

The observed stability behaviour can be interpreted through the statistical structure of the hybrid availability signal. Let the normalised solar and wind availability indices be denoted by $S(t)$ and $W(t)$, respectively, and define the hybrid availability signal as:

$$H(t;\alpha) = \alpha S(t) + (1-\alpha)W(t), \qquad \alpha \in [0,1] \qquad (11)$$

The variance of the hybrid signal can then be expressed as:

$$Var[H] = \alpha^2 Var[S] + (1-\alpha)^2 Var[W] + 2\alpha(1-\alpha)Cov[S,W] \qquad (12)$$

In regions characterised by seasonal wind–solar complementarity, the covariance term $Cov[S,W]$ is negative. Under this condition, $Var[H]$ becomes a convex quadratic function of α, admitting an interior minimum. This explains the existence of a variability-optimal hybrid configuration, which arises from the covariance structure of the underlying signals, particularly under conditions of negative covariance, rather than from technology-specific assumptions. The result therefore reflects a general statistical property of temporally anti-correlated resource pairs.

Transition intensity follows a fundamentally different mechanism. While variability depends on dispersion around the mean, transition intensity is governed by first differences of the availability signals. Solar availability typically evolves more smoothly, whereas wind availability is influenced by synoptic-scale variability and exhibits sharper temporal fluctuations. As a result, increasing the solar contribution reduces transition intensity more effectively, shifting the minimum towards higher values of α.

The separation between variability-optimal and transition-intensity-optimal configurations reflects the presence of distinct statistical mechanisms operating across temporal scales.

Consequently, wind–solar hybridisation does not admit a single universal optimum, but instead exhibits an intrinsic trade-off between variability reduction and transition smoothing.

This behaviour is not specific to the case study considered here, but arises from the general interaction between complementary resource signals. It is consistent with empirical evidence showing that temporal complementarity between wind and solar resources can generate stabilisation benefits and system-level value in hybrid configurations, [43], [44].

RESULTS

This section presents the results of the proposed framework across the Vlora case study and the multi-zonal configurations. All results are evaluated on consistently aggregated monthly time series, ensuring methodological comparability. The analysis proceeds from the characterisation of resource availability patterns to the evaluation of hybridisation effects and the identification of stability-relevant trade-offs across the mixing parameter space.

Resource availability signals and hybrid construction.

The analysis begins by examining the temporal structure of the normalised resource availability signals, which form the basis of the proposed hybridisation framework. Figure 3 presents the normalised monthly time series of solar availability $S(t)$, wind availability $W(t)$, and the corresponding hybrid availability signal $H(t)$ for the Vlora region over the period 2014–2024.

The individual resource signals exhibit a pronounced seasonal anti-phase behaviour, with solar availability peaking during summer months and wind availability dominating during winter. This temporal structure is consistent with Mediterranean climatic conditions and provides the underlying basis for hybridisation within the proposed framework. From a resource-level perspective, this anti-phased behaviour enables partial temporal compensation between the two signals, which is a necessary condition for variability reduction in the aggregated availability profile.

For illustrative purposes, the hybrid availability signal $H(t)$ is shown for a representative mixing parameter $\alpha = 0.5$, corresponding to equal contributions from the normalised solar and wind availability indices. This value is used solely as a neutral reference case for visual interpretation, while the full range $\alpha \in [0, 1]$ is systematically explored in the subsequent optimisation analysis. At this reference configuration, the hybrid signal exhibits a visibly smoother temporal profile, with reduced amplitude of deviations relative to the individual resource signals. This smoothing effect reflects the statistical interaction between the two availability signals and provides an initial indication of the variability-reduction potential that is analysed quantitatively in the following sections.

To assess the spatial robustness of these patterns, Table 1 presents the corresponding normalised monthly availability indices across three physiographic zones in Albania. The reported values correspond to dimensionless standardised anomalies (z-scores) of solar S(t) and wind W(t) availability, derived from ERA5 atmospheric reanalysis data for the period 2014–2024.

While Figure 3 illustrates the temporal dynamics at a single reference location, the multi-zonal data demonstrate that the seasonal anti-phase structure between solar and wind availability is consistently preserved across coastal, lowland, and mountainous regions.

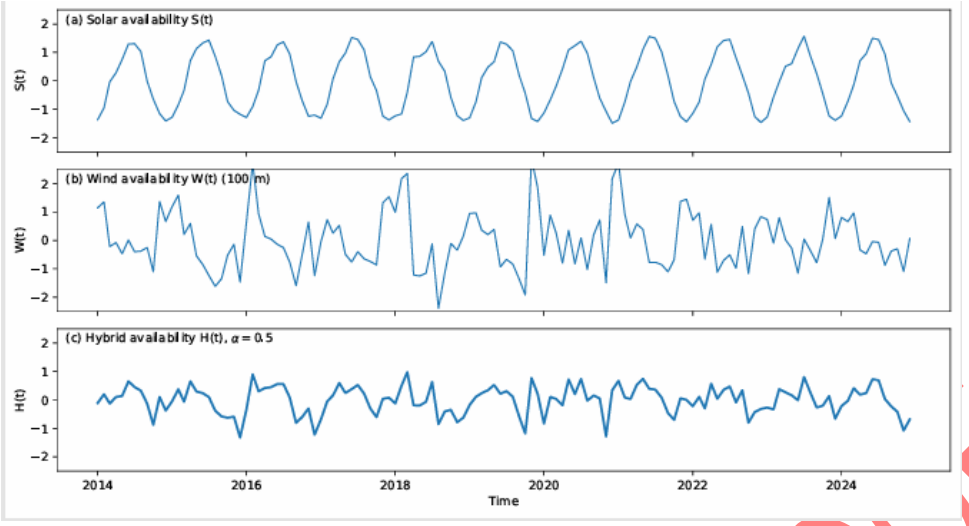

Figure 3. Normalised monthly solar $S\ (t)$, wind $W(t)$, and hybrid $H(t)$ availability signals for Vlora region (2014–2024). The hybrid signal is constructed using a representative mixing parameter $\alpha\ =\ 0.5$. The figure illustrates the seasonal anti-phase behaviour between solar and wind resources and the resulting smoothing effect in the hybrid availability signal.

Table 1. Normalised monthly solar $S(t)$ and wind $W(t)$ availability indices across the identified physiographic archetypes in Albania.

Month	Coastal Belt		Western Lowlands		Mountainous Area	
	S(t) [-]	W(t) [-]	S(t) [-]	W(t) [-]	S(t) [-]	W(t) [-]
January	0.657	0.897	0.851	0.613	0.409	0.252
February	0.944	0.892	0.798	0.648	0.504	0.466
March	0.780	0.981	0.648	0.731	0.394	0.506
April	0.912	0.844	0.774	0.665	0.521	0.489
May	0.955	0.801	0.812	0.689	0.566	0.533
June	0.972	0.756	0.845	0.612	0.590	0.498
July	0.978	0.701	0.856	0.584	0.612	0.472
August	0.981	0.688	0.862	0.573	0.624	0.465
September	0.948	0.782	0.821	0.661	0.585	0.522
October	0.905	0.865	0.778	0.712	0.532	0.578
November	0.701	0.902	0.589	0.768	0.422	0.642
December	0.662	0.910	0.853	0.784	0.415	0.655

Despite regional differences in magnitude associated with topographic and climatic variability, the persistence of this temporal structure indicates that wind–solar complementarity reflects a broader regional climatic characteristic rather than a site-specific feature. This consistency provides a basis for applying the proposed framework across heterogeneous resource conditions.

Importantly, the hybrid signals are constructed independently of assumptions regarding installed capacity, conversion efficiency, or system configuration. The results therefore represent purely resource-driven availability patterns within a technology-agnostic framework. This abstraction enables a consistent evaluation of integration-relevant temporal behaviour, which is quantified in the subsequent sections using variability, inter-period transition intensity, and demand-alignment metrics.

Variability reduction through wind–solar hybridisation.

Figure 4 presents a comparative assessment of variability and inter-period transition intensity for solar-only, wind-only, and hybrid availability signals, using a representative mixing parameter of α = 0.5, corresponding to equal contributions from the normalised solar and wind availability indices. The results show that the hybrid signal exhibits a substantially lower level of variability compared to the individual resource signals. Although the solar and wind availability indices display comparable dispersion following standardisation, their aggregation results in a pronounced attenuation of variability. In particular, the standard deviation of the hybrid signal is reduced by approximately 51% relative to the single-resource cases, indicating a strong variability-reduction effect of wind–solar hybridisation.

In addition to overall variability, Figure 4 also characterises inter-period transition behaviour, quantified as the mean absolute change between consecutive time steps. The hybrid configuration demonstrates a clear reduction in transition intensity, particularly relative to the wind-only case, which represents the most variable single resource. Specifically, the hybrid signal reduces transition intensity by approximately 49% compared to wind, indicating a significant mitigation of month-to-month fluctuations. This metric is evaluated at a monthly temporal resolution and should therefore be interpreted as inter-period variability rather than short-term operational dynamics.

Taken together, the reductions in variability (≈51%) and transition intensity (≈49%) indicate that wind–solar hybridisation is associated with a smoother and more temporally consistent availability profile. These results provide the quantitative basis for the subsequent sensitivity analysis, which examines how these improvements evolve as a function of the mixing parameter α. The corresponding numerical values for the Vlora case study are reported in Table 2, providing a quantitative reference for the reductions observed in Figure 4.

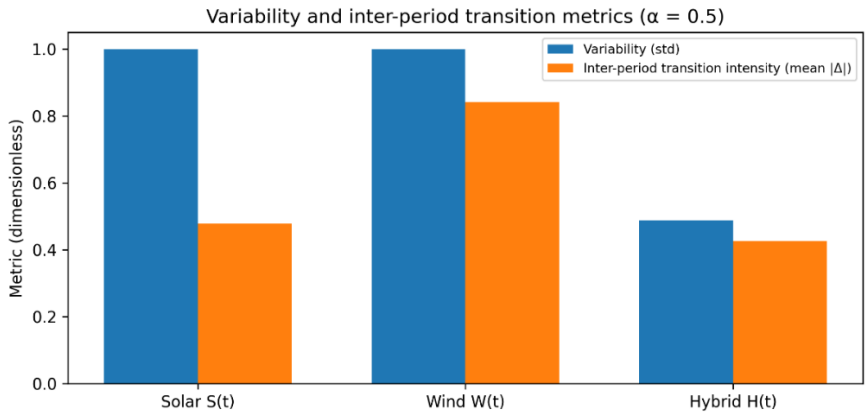

Figure 4. Comparison of variability (standard deviation) and inter-period transition intensity (mean absolute first-order difference, |Δ|) for normalised monthly solar, wind, and hybrid availability signals at a representative mixing parameter α = 0.5 (Vlora case study).

Table 2. Variability (σ) and transition intensity (mean $|\Delta|$) for solar-only, wind-only, and hybrid availability signals at $\alpha = 0.5$, including relative reductions compared to single-resource configurations.

Configuration	Variability (σ)	Transition Intensity (mean |Δ|)	Relative Reduction
Solar-only	1.00	0.48	–
Wind-only	1.00	0.84	–
Hybrid (α = 0.5)	0.49	0.43	~51%(variability), ~49% (transition)

Sensitivity to the mixing parameter α and integration stability trade-offs

The transition from single-resource availability signals to a hybrid wind–solar representation enables a continuous evaluation of integration-relevant temporal behaviour as a function of the mixing parameter α. To assess the robustness of these patterns across heterogeneous resource conditions, a sensitivity analysis is conducted for two key indicators: variability ($\sigma(H)$) and inter-period transition intensity.

As α increases from wind-dominated ($\alpha \rightarrow 0$) to solar-dominated ($\alpha \rightarrow 1$) regimes, the variability exhibits a pronounced convex profile, as illustrated in Figure 5. This behaviour reflects the quadratic dependence of $Var(H)$ on α derived in eq. (12) where the covariance term Cov(S, W) governs the existence of an interior minimum. Under conditions of negative covariance between wind and solar availability, variability is minimised at intermediate α values, indicating a variability-optimal hybrid configuration.

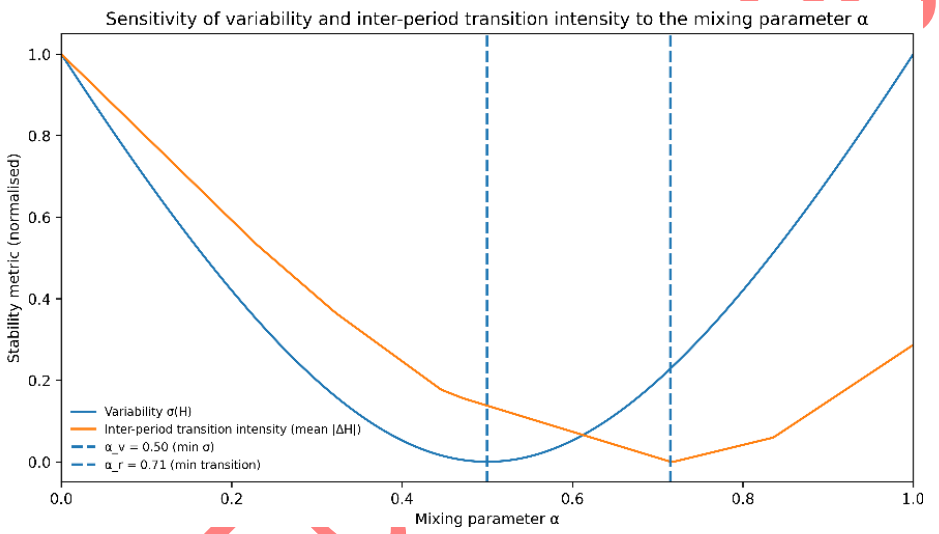

Figure 5. Sensitivity of variability and inter-period transition intensity to the mixing parameter α for the Vlora case study. Metrics are evaluated from the hybrid availability signal constructed using normalised monthly wind and solar indices. Variability is quantified as the standard deviation $\sigma(H)$, and inter-period transition intensity as the mean absolute first-order difference. Both metrics are rescaled using min–max normalisation for visual comparability. Vertical dashed lines indicate the optimal mixing parameters for variability (α_v) and transition intensity (α_r), highlighting the non-coincidence of optimal configurations.

Across the three physiographic archetypes (Coastal Belt, Western Lowlands, and Mountainous Area), the variability reaches its minimum at the specific monthly mixing configurations detailed in Table 3. While the exact values vary across regions and seasons, the overall convex structure is consistently preserved. A key result of the analysis is the non-coincidence of optimal configurations for variability and inter-period transition intensity. While variability is minimised at specific mixing ratios (e.g., $\alpha \approx 0.37$ for the Mountainous Area in December; Table 3), transition intensity generally reaches its minimum at higher solar contributions. This divergence reflects the presence of distinct statistical mechanisms governing dispersion and temporal transitions, leading to an inherent trade-off between long-term variability reduction and the smoothing of inter-period changes.

The sensitivity patterns further indicate that the response of the system to α is region-dependent. The Western Lowlands (including the Vlora reference site) exhibit a relatively broad minimum, suggesting a wider range of near-optimal configurations, particularly towards solar-dominated regimes (α approaching 0.9 in summer). In contrast, the Mountainous Area

shows a steeper sensitivity profile, where deviations from the optimal configuration result in a more rapid increase in transition intensity.

Importantly, the spatiotemporal distribution of α values (Table 3) indicates that no single hybrid configuration simultaneously optimises all integration-relevant criteria across seasons and regions. The identified α values should therefore be interpreted as resource-level balancing indicators, providing directional guidance for hybridisation strategies rather than prescriptive system design parameters.

Table 3. Monthly optimal values of the mixing parameter α across physiographic archetypes, indicating variability-minimising configurations.

Month	Coastal Belt	Western Lowlands	Mountainous Area
January	0.47	0.58	0.43
February	0.59	0.71	0.56
March	0.63	0.73	0.61
April	0.63	0.74	0.56
May	0.71	0.75	0.63
June	0.80	0.86	0.70
July	0.85	0.90	0.74
August	0.79	0.86	0.71
September	0.68	0.77	0.61
October	0.54	0.63	0.47
November	0.45	0.54	0.41
December	0.41	0.51	0.37

DISCUSSION

The results demonstrate that transitioning from single-resource representations to a hybrid wind–solar framework is associated with improved temporal consistency of renewable availability. Importantly, this smoothing effect should not be interpreted as a direct measure of system integration value, as it reflects statistical properties of resource availability rather than operational system performance or grid-level dynamics. By adopting a technology-agnostic perspective, the analysis isolates the intrinsic balancing potential of Albania's climatic resource patterns across different physiographic archetypes.

Sensitivity analysis and resource-demand alignment.

The sensitivity analysis reveals a non-linear response of integration-relevant temporal behaviour to the mixing parameter α. Variability ($\sigma(H)$) follows a convex profile across the full range $\alpha \in [0,1]$, reflecting the covariance-driven interaction between wind and solar availability.

Across all archetypes, variability reaches a minimum at intermediate α values (Table 3), reflecting the partial compensation of individual resource fluctuations rather than their complete cancellation.

A key finding is the non-coincidence of optimal configurations for variability and inter-period transition intensity. While variability is minimised at intermediate α values, transition intensity generally requires a higher solar contribution to reach its minimum. This trade-off implies that hybrid system optimisation cannot be defined by a single objective, but must instead be aligned with the dominant temporal and integration constraints of the system.

The observed patterns across the Coastal Belt, Western Lowlands, and Mountainous Area suggest a consistent regional response of hybrid availability to the mixing parameter α. The Western Lowlands exhibit a broader tolerance for solar-dominated configurations, with near-

optimal regimes extending towards higher α values (approaching 0.90 in summer). In contrast, the Mountainous Area shows a stronger dependence on wind availability, with optimal configurations shifting towards lower α values (e.g., around 0.37 in winter). This regional differentiation indicates that hybridisation behaviour depends on the relative structure and seasonal dynamics of the underlying resource signals.

To assess practical relevance, the hybrid availability signal was compared with normalised monthly electricity demand for the Vlora region. Solar availability aligns with summer demand peaks, while wind availability dominates during winter months, indicating a complementary seasonal structure relative to demand. The hybrid configuration moderates these opposing seasonal patterns, resulting in a smoother availability profile that more closely follows demand.

The optimal α values identified in Table 3 should therefore be interpreted as resource-level balancing indicators. Rather than representing a fixed solution, they provide a flexible reference for aligning hybrid configurations with specific integration priorities and seasonal demand conditions.

Although the mixing parameter α is intentionally defined as a dimensionless analytical weighting factor rather than a direct representation of installed capacity shares, the identified α ranges may still provide useful insight for planning-oriented hybridisation strategies. In this context, lower α values indicate wind-leaning hybrid regimes, whereas higher α values correspond to increasingly solar-dominated configurations. The resulting stability-optimal ranges therefore provide directional guidance regarding the relative balance between wind and solar availability under different climatic and integration-related conditions. From a planning perspective, these results may support early-stage screening and the prioritisation of candidate hybrid configurations before applying detailed techno-economic optimisation or operational modelling. However, translating the identified α values into real-world system design would require further modelling of installed capacities, technology performance, storage integration, grid constraints, and dispatch behaviour.

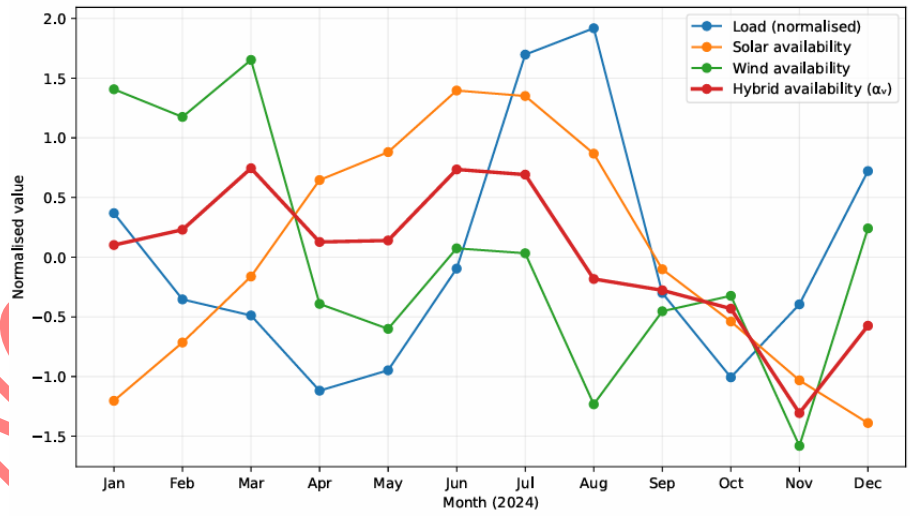

Figure 6. Normalised monthly electricity demand and renewable availability signals for the Vlora region (2024).

Demand-aware residual analysis and balancing stress.

To quantify the seasonal alignment patterns, demand–availability residuals are introduced as a proxy for resource-level temporal mismatch. This metric provides a planning-oriented indicator of the magnitude and persistence of mismatches, without representing operational dispatch (see Supplementary Material S6). The analysis shows a clear reduction in residual variability under hybrid configurations compared to solar-only and wind-only cases. This reduction suggests a closer temporal alignment between aggregated renewable availability and

demand patterns. In the Vlora case study, the hybrid configuration constructed using the variability-optimal mixing parameter $\alpha\_v = 0.50$ reduces residual dispersion, thereby moderating the overall mismatch magnitude. Figure 7 summarises this effect by comparing the standard deviation of the residual proxy across the three configurations. The hybrid case exhibits the lowest residual variability, reflecting a reduced spread of mismatch values over the annual cycle.

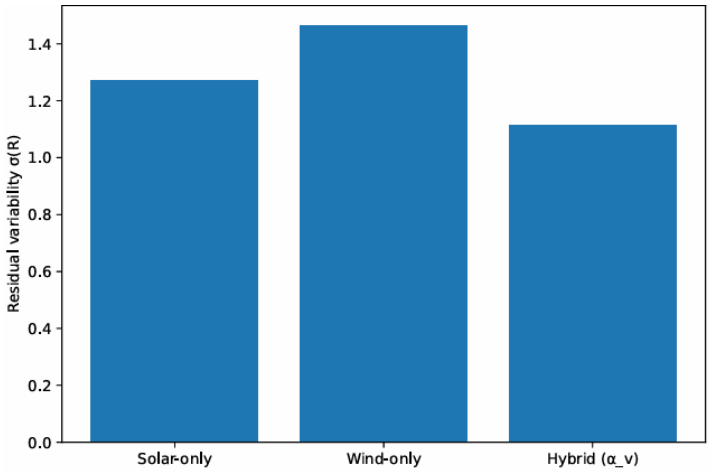

Figure 7. Residual variability (standard deviation of the demand–availability residual proxy) for solar-only, wind-only, and hybrid configurations ($\alpha\_v = 0.50$) in the Vlora region (2024), evaluated at monthly resolution. The hybrid configuration exhibits reduced mismatch dispersion relative to single-resource cases.

The temporal evolution of the residual proxy further illustrates this behaviour. Solar-only configurations exhibit large positive residuals during winter, while wind-only configurations show significant mismatches during summer (see Figure 8**)**. The hybrid signal attenuates both the amplitude and persistence of these deviations, maintaining a more balanced profile over the annual cycle.

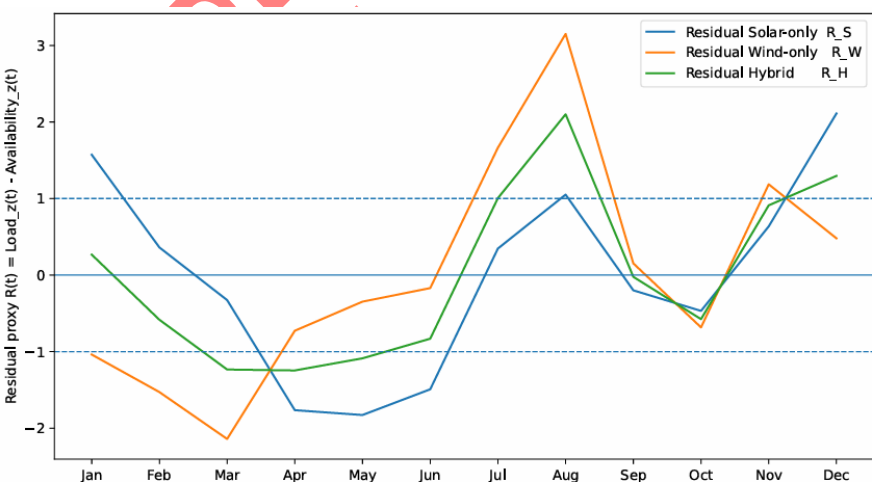

Figure 8. Monthly demand–availability residual proxy for solar only, wind-only, and hybrid configurations (Vlora, 2024).

Overall, the results presented in Figure 6, Figure 7, Figure 8 demonstrate that wind–solar hybridisation improves demand–availability alignment at the monthly scale, primarily through the reduction of seasonal mismatch patterns. These findings are derived without reliance on dispatch modelling or technology-specific assumptions, supporting the use of the residual proxy as a transferable tool for early-stage integration assessment.

Implications of stability trade-offs for system planning and demand matching.

The identification of distinct optimal mixing parameters for variability and inter-period transition intensity minimisation reveals an inherent trade-off in wind–solar hybrid integration. Variability is minimised at intermediate mixing ratios ($\alpha_v \approx 0.5$), while transition intensity reaches its minimum at higher solar contributions ($\alpha_r \approx 0.7$). This non-coincidence indicates that no single configuration simultaneously optimises all integration-relevant criteria, and that optimality is inherently dependent on the temporal scale and system objective.

From a planning perspective, this distinction has direct implications. Variability reduction primarily relates to seasonal and intra-annual balancing considerations, influencing aspects such as supply consistency and the potential role of storage. In contrast, inter-period transition intensity reflects the smoothness of temporal changes at the resolution considered in the analysis. Hybrid configurations should therefore be selected based on the dominant integration constraint rather than a universal optimisation target.

In this study, the demand-aware residual analysis is evaluated using the variability-optimal mixing parameter (α_v), ensuring consistency with the monthly temporal resolution of the demand data. The resulting reduction in residual variability is consistent with a closer alignment between renewable availability and demand patterns under the examined conditions. By explicitly identifying multiple optimal mixing regimes, the proposed framework avoids prescribing a fixed hybrid configuration. Instead, it characterises a continuum of trade-offs that can inform planning decisions under uncertainty. This separation between resource-driven stability evaluation and demand-aware assessment provides a transparent, technology-agnostic basis for analysing hybrid renewable integration in regions with strong seasonal complementarity.

Limitations and scope.

The proposed framework is designed as a planning-stage, technology-neutral screening tool and therefore deliberately abstracts from detailed operational power system dynamics. The use of normalised availability indices reflects relative resource availability rather than physical electricity production, installed capacity, conversion efficiency, or dispatch feasibility, and the analysis focuses on planning-oriented behaviour instead of simulating real-time power flows or operational constraints. The use of monthly temporal aggregation may smooth short-term variability patterns that are relevant for operational system analysis; however, these dynamics are beyond the scope of the present planning-oriented framework.

Within this scope, the inter-period transition metric captures variability at a monthly resolution and should be interpreted as a proxy for medium-term temporal changes rather than an operational ramping constraint. Similarly, the demand-aware residual analysis serves as an indicative measure of temporal alignment between renewable availability and regional demand patterns, rather than a direct representation of physical residual load. These abstractions are consistent with the planning-oriented objective of the framework, which focuses on identifying resource-driven integration behaviour independently of system-specific assumptions such as unit commitment, reserve activation, or flexibility constraints.

Accordingly, the framework is positioned as a complementary pre-modelling diagnostic, providing a transparent and computationally efficient basis for identifying suitable hybridisation configurations prior to technology-specific implementation.

Future work may extend the analysis to sub-daily temporal resolutions, incorporate additional renewable resources, and integrate the proposed indicators into detailed system-level models. More broadly, the results highlight that wind–solar complementarity is better understood as a set of distinct integration mechanisms operating across temporal scales, rather than a single aggregated benefit. The non-coincidence of optimal configurations indicates that hybrid system performance is inherently multi-dimensional and cannot be fully characterised

by a single metric, reinforcing the need for multi-dimensional assessment in planning-oriented studies.

CONCLUSIONS

This study demonstrates that wind–solar hybridisation is associated with improved integration-relevant temporal behaviour by reducing both long-term variability and inter-period transition intensity relative to single-resource configurations. By formulating renewable availability using normalised signals, the analysis shows that resource complementarity can translate into measurable integration value when wind and solar are jointly considered.

The results identify distinct optimal mixing regimes for different integration objectives. Long-term variability is minimised at balanced wind–solar contributions ($\alpha_v \approx 0.5$), whereas transition intensity minimisation occurs at higher solar shares. This separation implies that no single hybrid configuration simultaneously optimises all criteria, and that optimality depends on the temporal scale of interest. By introducing a demand-aware residual framework, the study further indicates that the variability-optimal configuration is associated with a closer temporal alignment between renewable availability and electricity demand. This effect arises primarily from reducing the persistence and magnitude of seasonal mismatches rather than eliminating isolated extremes.

The main contribution lies in formalising how resource complementarity gives rise to distinct and non-coincident integration mechanisms, linking variability reduction, transition behaviour, and demand alignment within a unified analytical framework.

Because the framework is expressed in terms of normalised availability signals and generalised indicators, it can be extended beyond wind–solar systems to other combinations of temporally complementary resources, providing a transferable basis for early-stage planning and hybrid integration assessment.

The analysis is conducted at a monthly resolution, consistent with the planning-oriented scope of the study. Higher-resolution data are used to ensure robustness, while the results remain focused on medium-term temporal behaviour rather than short-term operational dynamics.

From a practical perspective, the framework serves as a pre-modelling screening tool, enabling the identification of favourable hybridisation ranges and explicit trade-offs prior to applying detailed capacity expansion or dispatch models. This supports the prioritisation of candidate configurations and reduces the solution space in early-stage planning.

Future work may extend the framework to higher temporal resolutions, incorporate additional renewable resources, or integrate these indicators within more detailed system models.

AUTHORSHIP CONTRIBUTION

Miranda Halili contributed to the literature review, conceptual development of the study, methodological framework, data collection and analysis, and manuscript preparation and revision.

Valbona Muda, Driada Mitrushi, and Fjorela Verore contributed through scientific discussion, interpretation of results, and review of the manuscript. All authors approved the final version.

CONFLICT OF INTEREST

The authors declare no conflict of interest.

DATA AVAILABILITY

The datasets analysed during the current study are available from the Copernicus Climate Data Store (CDS): https://cds.climate.copernicus.eu

ETHICS STATEMENT

This study does not involve human participants or animal subjects.

ACKNOWLEDGMENT

The authors acknowledge the institutional support provided by the University of Vlora "Ismail Qemali" and the Polytechnic University of Tirana during the development of this study.

REFERENCES

1. P. D. Lund, J. Lindgren, J. Mikkola, and J. Salpakari, 'Review of energy system flexibility measures to enable high levels of variable renewable electricity', *Renew. Sustain. Energy Rev.*, vol. 45, pp. 785–807, May 2015, https://doi.org/10.1016/j.rser.2015.01.057.
2. M. M. Rahman, S. H. Dadon, M. He, M. Giesselmann, and M. M. Hasan, 'An Overview of Power System Flexibility: High Renewable Energy Penetration Scenarios', *Energies*, vol. 17, no. 24, p. 6393, Dec. 2024, https://doi.org/10.3390/en17246393.
3. W.-P. Schill and A. Zerrahn, 'Long-run power storage requirements for high shares of renewables: Results and sensitivities', *Renew. Sustain. Energy Rev.*, vol. 83, pp. 156–171, Mar. 2018, https://doi.org/10.1016/j.rser.2017.05.205.
4. P. Das, A. Kanudia, R. Bhakar, and J. Mathur, 'Intra-regional renewable energy resource variability in long-term energy system planning', *Energy*, vol. 245, p. 123302, Apr. 2022, https://doi.org/10.1016/j.energy.2022.123302.
5. M. Emmanuel, K. Doubleday, B. Cakir, M. Marković, and B.-M. Hodge, 'A review of power system planning and operational models for flexibility assessment in high solar energy penetration scenarios', *Sol. Energy*, vol. 210, pp. 169–180, Nov. 2020, https://doi.org/10.1016/j.solener.2020.07.017.
6. A. M. Iung, F. L. Cyrino Oliveira, and A. L. M. Marcato, 'A Review on Modeling Variable Renewable Energy: Complementarity and Spatial–Temporal Dependence', *Energies*, vol. 16, no. 3, p. 1013, Jan. 2023, https://doi.org/10.3390/en16031013.
7. G. Parrado-Hernando, F. Frechoso-Escudero, and L. J. Miguel González, 'Method to Model the Hourly Variability of Renewable Energy Sources in Integrated Assessment Models', *J. Sustain. Dev. Energy Water Environ. Syst.*, vol. 12, no. 1, pp. 1–25, Mar. 2024, https://doi.org/10.13044/j.sdewes.d11.0481.
8. X. Costoya, M. deCastro, D. Carvalho, and M. Gómez-Gesteira, 'Assessing the complementarity of future hybrid wind and solar photovoltaic energy resources for North America', *Renew. Sustain. Energy Rev.*, vol. 173, p. 113101, Mar. 2023, https://doi.org/10.1016/j.rser.2022.113101.
9. W.-B. Chen, 'Assessing global land-based solar–wind complementarity using high-resolution climate reanalysis for hybrid renewable energy design', *Energy Convers. Manag.*, vol. 343, p. 120267, Nov. 2025, https://doi.org/10.1016/j.enconman.2025.120267.
10. J. López Prol, F. De Llano Paz, A. Calvo-Silvosa, S. Pfenninger, and I. Staffell, 'Wind-solar technological, spatial and temporal complementarities in Europe: A portfolio approach', *Energy*, vol. 292, p. 130348, Apr. 2024, https://doi.org/10.1016/j.energy.2024.130348.
11. F. Lv and H. Tang, 'Assessing the impact of climate change on the optimal solar–wind hybrid power generation potential in China: A focus on stability and complementarity', *Renew. Sustain. Energy Rev.*, vol. 212, p. 115429, Apr. 2025, https://doi.org/10.1016/j.rser.2025.115429.
12. T. H. Soukissian, F. E. Karathanasi, and D. K. Zaragkas, 'Exploiting offshore wind and solar resources in the Mediterranean using ERA5 reanalysis data', *Energy Convers. Manag.*, vol. 237, p. 114092, June 2021, https://doi.org/10.1016/j.enconman.2021.114092.

13. A. Beluco, P. K. De Souza, and A. Krenzinger, 'A dimensionless index evaluating the time complementarity between solar and hydraulic energies', *Renew. Energy*, vol. 33, no. 10, pp. 2157–2165, Oct. 2008, https://doi.org/10.1016/j.renene.2008.01.019.

14. J. Jurasz, F. A. Canales, A. Kies, M. Guezgouz, and A. Beluco, 'A review on the complementarity of renewable energy sources: Concept, metrics, application and future research directions', *Sol. Energy*, vol. 195, pp. 703–724, Jan. 2020, https://doi.org/10.1016/j.solener.2019.11.087.

15. J. L. Muñoz-Pincheira, L. Salazar, F. Sanhueza, and A. Lüer-Villagra, 'Temporal Complementarity Analysis of Wind and Solar Power Potential for Distributed Hybrid Electric Generation in Chile', *Energies*, vol. 17, no. 8, p. 1890, Apr. 2024, https://doi.org/10.3390/en17081890.

16. E. Jonasson and I. Temiz, 'Evaluating complementarity: A review of metrics and their implications for hybrid renewable energy systems', *Renew. Sustain. Energy Rev.*, vol. 226, p. 116422, Jan. 2026, https://doi.org/10.1016/j.rser.2025.116422.

17. E. Ejuh Che, K. Roland Abeng, C. D. Iweh, G. J. Tsekouras, and A. Fopah-Lele, 'The Impact of Integrating Variable Renewable Energy Sources into Grid-Connected Power Systems: Challenges, Mitigation Strategies, and Prospects', *Energies*, vol. 18, no. 3, p. 689, Feb. 2025, https://doi.org/10.3390/en18030689.

18. T. A. Hamed and A. Alshare, 'Environmental Impact of Solar and Wind energy- A Review', *J. Sustain. Dev. Energy Water Environ. Syst.*, vol. 10, no. 2, pp. 1–23, June 2022, https://doi.org/10.13044/j.sdewes.d9.0387.

19. H. Wu and S. R. West, 'Co-optimisation of wind and solar energy and intermittency for renewable generator site selection', *Heliyon*, vol. 10, no. 5, p. e26891, Mar. 2024, https://doi.org/10.1016/j.heliyon.2024.e26891.

20. S. A. A., M. Child, U. Caldera, C. Breyer, and LUT University, Yliopistonkatu 34, 53850 Lappeenranta, Finland, 'Exploiting wind-solar resource complementarity to reduce energy storage need', *AIMS Energy*, vol. 8, no. 5, pp. 749–770, 2020, https://doi.org/10.3934/energy.2020.5.749.

21. S. Ben Mabrouk, S. Favuzza, D. La Cascia, F. Massaro, and G. Zizzo, 'Energy Management of a Hybrid Photovoltaic-Wind System with Battery Storage: A Case Report', *J. Sustain. Dev. Energy Water Environ. Syst.*, May 2019, https://doi.org/10.13044/j.sdewes.d6.0233.

22. M. Al-Rasheedi and M. Al-Khayat, 'Assessing wind and solar energy complementarity using novel metrics based on residual load profiles', *Energy*, vol. 335, p. 138107, Oct. 2025, https://doi.org/10.1016/j.energy.2025.138107.

23. T. H. Ruggles and K. Caldeira, 'Wind and solar generation may reduce the inter-annual variability of peak residual load in certain electricity systems', *Appl. Energy*, vol. 305, p. 117773, Jan. 2022, https://doi.org/10.1016/j.apenergy.2021.117773.

24. H. Hersbach *et al.*, 'The ERA5 global reanalysis', *Q. J. R. Meteorol. Soc.*, vol. 146, no. 730, pp. 1999–2049, July 2020, https://doi.org/10.1002/qj.3803.

25. C3S, 'ERA5 hourly data on single levels from 1940 to present', 2018. https://cds.climate.copernicus.eu/doi/10.24381/cds.adbb2d47 (accessed Jan. 10, 2024).

26. 'QGIS Geographic Information System', 2023. https://qgis.org (accessed Jan. 15, 2026).

27. Natural Earth (corporate author), 'Admin 0 – Countries (1:10m cultural vectors)', 2023. https://www.naturalearthdata.com (accessed Jan. 22, 2026).

28. Chatfield, C., *The Analysis of Time Series: An Introduction*, 6th ed. Boca Raton, FL, USA: Chapman & Hall/CRC, 2004.

29. H. C. Bloomfield, C. M. Wainwright, and N. Mitchell, 'Characterizing the variability and meteorological drivers of wind power and solar power generation over Africa', *Meteorol. Appl.*, vol. 29, no. 5, p. e2093, Sept. 2022, https://doi.org/10.1002/met.2093.

30. S. Sterl, S. Liersch, H. Koch, N. P. M. V. Lipzig, and W. Thiery, 'A new approach for assessing synergies of solar and wind power: implications for West Africa', *Environ. Res. Lett.*, vol. 13, no. 9, p. 094009, Sept. 2018, https://doi.org/10.1088/1748-9326/aad8f6.

31. M. M. Miglietta, T. Huld, and F. Monforti-Ferrario, 'Local Complementarity of Wind and Solar Energy Resources over Europe: An Assessment Study from a Meteorological Perspective', *J. Appl. Meteorol. Climatol.*, vol. 56, no. 1, pp. 217–234, Jan. 2017, https://doi.org/10.1175/JAMC-D-16-0031.1.

32. D. Tong, D. J. Farnham, L. Duan, Q. Zhang, N. S. Lewis, K. Caldeira, and S. J. Davis, 'Geophysical constraints on the reliability of solar and wind power worldwide', *Nat. Commun.*, vol. 12, no. 1, p. 6146, Oct. 2021, https://doi.org/10.1038/s41467-021-26355-z.

33. N. Passalis, C. N. Dimitriadis, and M. C. Georgiadis, 'Residual adaptive input normalization for forecasting renewable energy generation in multiple countries', *Pattern Recognit. Lett.*, vol. 196, pp. 52–58, Oct. 2025, https://doi.org/10.1016/j.patrec.2025.05.008.

34. A. Martinez and G. Iglesias, 'Hybrid wind-solar energy resources mapping in the European Atlantic', *Sci. Total Environ.*, vol. 928, p. 172501, June 2024, https://doi.org/10.1016/j.scitotenv.2024.172501.

35. P. J. Brockwell and R. A. Davis, *Introduction to time series and forecasting*, 3rd ed. Cham, Switzerland: Springer, 2016.

36. D.-A. Ciupăgeanu, G. Lăzăroiu, and L. Barelli, 'Wind energy integration: Variability analysis and power system impact assessment', *Energy*, vol. 185, pp. 1183–1196, Oct. 2019, https://doi.org/10.1016/j.energy.2019.07.136.

37. J. D. Hamilton, *Time series analysis*. Princeton, N.J: Princeton University Press, 1994.

38. R. H. Shumway and D. S. Stoffer, *Time Series Analysis and Its Applications: With R Examples*, 4th edn. Cham, Switzerland: Springer International Publishing, 2017.

39. G. D'Amico, F. Petroni, and S. Vergine, 'Ramp Rate Limitation of Wind Power: An Overview', *Energies*, vol. 15, no. 16, p. 5850, Aug. 2022, https://doi.org/10.3390/en15165850.

40. M. Al-Rasheedi and M. Al-Khayat, 'Assessing wind and solar energy complementarity using novel metrics based on residual load profiles', *Energy*, vol. 335, p. 138107, Oct. 2025, https://doi.org/10.1016/j.energy.2025.138107.

41. J. M. Wilczak, D. B. Kirk-Davidoff, H. Bloomfield, C. Bracken, and J. Sharp, 'Wind and solar energy droughts: Potential impacts on energy system dynamics and research needs', *J. Renew. Sustain. Energy*, vol. 17, no. 2, p. 022301, Mar. 2025, https://doi.org/10.1063/5.0253058.

42. Paul Embrechts, Claudia Klüppelberg, Thomas Mikosch, *Modelling Extremal Events for Insurance and Finance*. Berlin, Germany: Springer, 1997.

43. D. Harrison-Atlas, C. Murphy, A. Schleifer, and N. Grue, 'Temporal complementarity and value of wind-PV hybrid systems across the United States', *Renew. Energy*, vol. 201, pp. 111–123, Dec. 2022, https://doi.org/10.1016/j.renene.2022.10.060.

44. X. Yuan, Y. Wei, and H. Yang, 'Wind-solar complementarity in the Northwest Pacific: Implications for renewable energy planning and policy guidance', *Appl. Energy*, vol. 401, p. 126600, Dec. 2025, https://doi.org/10.1016/j.apenergy.2025.126600.